Mechanism of Oxidation of (olefin)Rh^I and -Ir^I Complexes by H_2O_2

Peter H. M. Budzelaar*[a] and Arno N. J. Blok[a]

Keywords: Density functional calculations / Iridium / Oxidation / Oxygenation / Rhodium

A DFT study of the oxidation of (tpa)$M^I(C_2H_4)^+$ and (dpa-R)M^I(cod)$^+$ complexes (M = Rh, Ir) by H_2O_2 indicates that the reaction starts with heterolytic cleavage of the peroxide O–O bond, leading to M^{III}(olefin)$(OH)^{2+}$ species. These can then undergo cyclisation, followed by deprotonation to oxetanes. In the oxidation of COD complexes, further cyclisation to internal ethers has a modest barrier, and the observed products (ethers for Rh, oxetanes for Ir) are suggested to be the thermodynamic ones.

Introduction

The oxidation of hydrocarbons at transition metal centres comprises a class of important yet poorly understood reactions. In addition to the more traditional organometallic reaction types, single-electron transfer steps and radical intermediates have to be considered. Moreover, oxidations are highly exothermic and often involve a cascade of elementary steps. These complications make the rational design and control of such reactions difficult and point to the need for a more detailed mechanistic understanding.

Still, not all oxidation reactions need necessarily be very complicated. Several years ago, De Bruin discovered the first clean example of the oxidation of a rhodium-coordinated ethene to an oxetane by H_2O_2 (Scheme 1).[1]

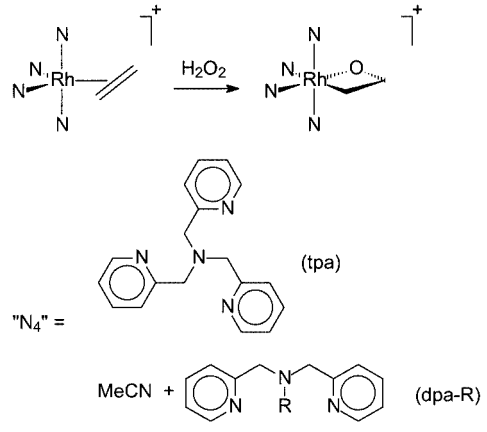

Scheme 1. Oxetane formation from ethene complexes and H_2O_2

Since then, this chemistry has been extended to cover also a few Ir examples, a few other N-donor ligands, propene and cyclooctadiene (COD).[2–5] In addition, the initial oxetane products have been converted into amido-substituted alkyl compounds, formylmethyl groups or acetaldehyde (Scheme 2).[6–8]

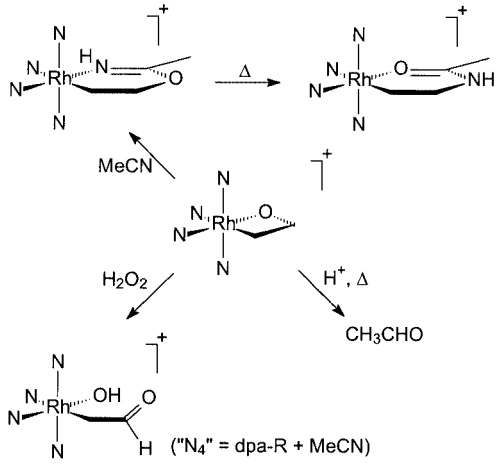

Scheme 2. Reactivity of oxarhodetanes

For COD the chemistry is somewhat more complex, since the second double bond can also participate in the oxygenation reaction, leading to internal ethers (Scheme 3). Depending on the metal, various isomeric ethers (Rh) or oxetanes (Ir) have been observed; in some cases, similar products have been observed in the oxidation of COD complexes by dioxygen (O_2).[3,9–11] It is not yet clear whether the observed isomers represent thermodynamic or kinetic products. In any case, they eventually rearrange to hydroxy-enediyl complexes.[2–4,9]

[a] Metal-Organic Chemistry, University of Nijmegen, Toernooiveld 1, 6525 ED Nijmegen, The Netherlands
Fax: (internat.) + 31-24-355-3450
E-mail: budz@sci.kun.nl

Supporting information for this article is available on the WWW under http://www.eurjic.org or from the author.

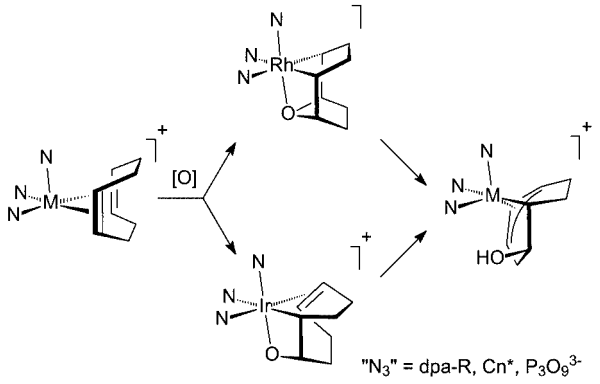

Scheme 3. Oxygenation of COD complexes

We have now studied the oxidation by H_2O_2 using DFT methods. For the initial oxidation step, three alternatives were considered, as summarised in Scheme 4: (*a*) concerted O−O bond breaking and Rh−O/C−O bond formation, followed by elimination of water; (*b*) heterolytic O−O cleavage, and then either (*b1*) deprotonation to an oxo complex, followed by cyclisation to an oxetane, or (*b2*) cyclisation to a protonated oxetane, followed by loss of the proton.

These reactions were studied for (tpa)M$(C_2H_4)^+$ complexes (M = Rh, Ir) as well as (dpa)M$(cod)^+$, (dpa-Me)M$(cod)^+$ (dpa-Me being a generic model for *N*-alkyl-substituted dpa ligands) and (tpa)M$(cod)^+$ (to explicitly include the possibility of a dangling picolyl group participating in the chemistry). For the COD complexes, interconversions between the various isomeric oxetane and ether products were investigated as well.

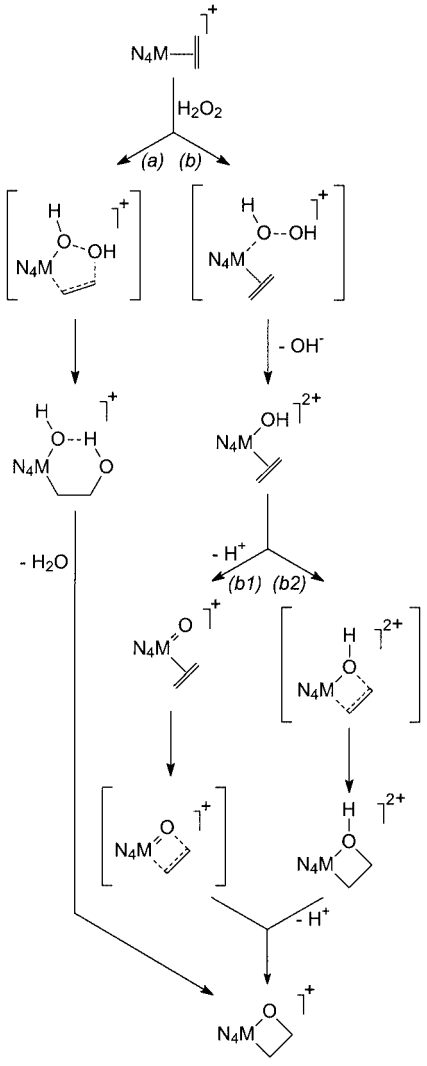

Scheme 4. Alternative mechanisms (*a*, *b1*, *b2*) for H_2O_2 oxidation of olefin complexes

Results and Discussion

Initial Attack of H_2O_2

Figure 1 shows the energy profiles for approach of H_2O_2 and $H_2O_2{\cdot}H_2O$ to (tpa)Rh$(C_2H_4)^+$ *cis* to the amine group [similar curves have been calculated for the *trans* approach and the corresponding reactions of (dpa)Rh$(cod)^+$ and (dpa-Me)Rh$(cod)^+$; see Supporting Information]. Starting from a weakly bound complex, the initial approach of the oxygen atom to the metal centre is slowly uphill in all cases. This is unsurprising, given the coordinatively saturated (18 e) nature of the metal centre. If only an isolated H_2O_2 molecule is used (Figure 1, diamonds), the approach stays repulsive up until fairly short M−O distances. The energy then goes down suddenly,[12] but the path does not lead to a protonated oxetane and separate OH^-, which would be too high in energy. Instead, a neighbouring acidic proton is immediately abstracted by the nascent OH^- group. Depending on the system, this can be the NH proton of dpa, a picolyl CH_2 proton of dpa or tpa, or the proton left on the OH group that was transferred to the metal atom. If a molecule of water is added, it hydrogen-bonds to H_2O_2. Now, on approach of an H_2O_2 oxygen atom to the metal atom the energy starts to go down already at longer M−O distances (Figure 1, squares), resulting in a marginally lower barrier.[12] For approach of both H_2O_2 and $H_2O_2{\cdot}H_2O$, the first step of the reaction appears to be heterolytic O−O cleavage, to form an OH^- ion (strongly stabilized by water if present) and an oxidized M^{III}(olefin)$(OH)^{2+}$ species. In practice, the H_2O_2 oxidation reactions always involve water and excess H_2O_2 able to sta-

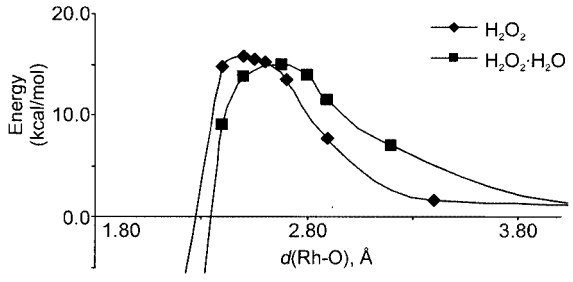

Figure 1. Potential-energy curve [kcal/mol] for approach of H_2O_2 or $H_2O_2{\cdot}H_2O$ to (tpa)Rh$(C_2H_4)^+$, *cis* to the amine nitrogen atom

bilize this nascent OH^-,[1−5] so easy heterolytic cleavage, assisted by hydrogen bonding, would be expected.

The calculated transition state (Figure 2) appears to be early, since the Rh−O distance (2.680 Å) is quite long. The barrier is mainly caused by the lateral movement of the coordinated ethene and the lengthening of the two in-plane Rh−N bonds, i.e. H_2O_2 displaces a nitrogen donor ligand and the Rh centre avoids a 20-electron surrounding. However, at the transition state the O−O bond is already elongated significantly relative to free $H_2O_2{\cdot}H_2O$ (1.465 Å). The barrier of about 15 kcal/mol (25 kcal/mol relative to the separated reactants) corresponds to a reaction that would be fast at room temperature. The results for Ir and for (dpa)M(cod)$^+$ and (dpa-Me)M(cod)$^+$ are very similar.

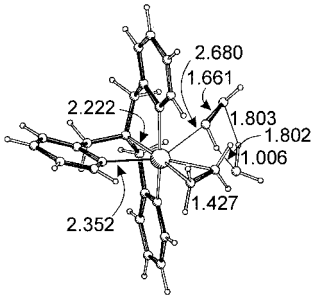

Figure 2. Calculated transition state for attack of $H_2O_2{\cdot}H_2O$ on (tpa)Rh$(C_2H_4)^+$ *cis* to the amine nitrogen atom; bond lengths in Å

The above constitutes the first step of variations (*b1*)and (*b2*) of Scheme 4. We have also considered variation (*a*) in which the nascent OH^- immediately attacks the olefin in a concerted manner. Despite extensive searches, no transition state for such an approach could be located; we conclude that no direct single-step reaction path exists. It remains possible that OH^- would first be lost and then attacks the olefin in a separate step. However, in that case approach to the olefin would be expected *trans* to the metal atom, and this would not lead to the COD oxidation products observed experimentally. In any case, it is not clear why, if route (*a*) were followed, the initially formed $M^{III}(OH)(CH_2CH_2OH)^{2+}$ complex would quickly rearrange to the (strained) oxetane observed experimentally. For these reasons, possibility (*a*) was not considered further.

Stereochemistry of H_2O_2 Attack

We assume that, once an M−O bond has been formed, the coordination chemistry around the metal atom is "frozen". This seems reasonable, since from that point on the complexes are octahedral ML_6 d^6 species and hence rather inert. Therefore, the final product distribution should reflect the stereochemistry of the initial H_2O_2 attack.

For oxidation of (tpa)Rh$(C_2H_4)^+$ by $H_2O_2{\cdot}H_2O$, we calculate a marginal preference (0.2 kcal/mol) for attack *cis* to the amine group. This agrees qualitatively with the stereochemistry observed experimentally, although the absence of any observable *trans* product[7] suggests that the real stereo preference is significantly higher than we calculate.

For oxidation of (dpa-Me)Rh(cod)$^+$ by $H_2O_2{\cdot}H_2O$, we calculate a similarly small preference (0.6 kcal/mol) for attack *cis* to the amine group, which corresponds to an expected *cis*/*trans* ratio of 3:1 at 0 °C. Experimentally, De Bruin observed a ratio of ca. 5:1 at room temperature and "selective" *cis* attack at −10 °C, which can be taken as reasonable agreement. The calculated *cis* preference is much larger (2.6 kcal/mol) for the oxidation of (dpa)Rh(cod)$^+$, where an additional hydrogen bond is formed between the auxiliary water molecule and the ligand NH group in the *cis*-attack transition state. It is not clear whether this is relevant to the "real" oxidation reaction, since there more water molecules would be present and the NH group would be involved in hydrogen bonding for *both* stereochemistries. In any case, the experimentally observed stereochemistry is indeed almost quantitatively *cis* to amine group for dpa-type ligands without a substituent at the amine nitrogen atom.

Formation of the First C−O Bond

Of the remaining variations (*b1* and *b2*), our results make the former one rather unlikely. The oxo intermediate in this mechanism is very high in energy. Its formation from the [(olefin)M^{I}]$^+$ complex and H_2O_2 is virtually thermoneutral, whereas the presumed intermediate hydroxo complex is about 40 kcal/mol lower in energy. The low stability of the oxo species is due to its lack of M−O π-bonding.[13] Thus, it is better represented by the zwitterionic M^+-O^- structure. Such an oxo complex is a very strong base, about 40 kcal/mol stronger than the final oxetane product. If it were formed at all, it would quickly cyclize to the oxetane; the calculated barrier for olefin insertion is negligible (1−2 kcal/mol).

In the second variation (*b2*), intramolecular nucleophilic attack of the OH group on the coordinated olefin has a modest barrier in all cases (5−15 kcal/mol). Thus, this represents a reasonable path for C−O bond formation. Subsequent loss of H^+ should also be easy, given the +2 charge of the complex. Therefore, we believe this path to be the more reasonable one, although, given the rough nature of our "solvation correction" (see Exp. Sect.) (*b1*) cannot be ruled out. Figure 3 shows the ring-closure transition state

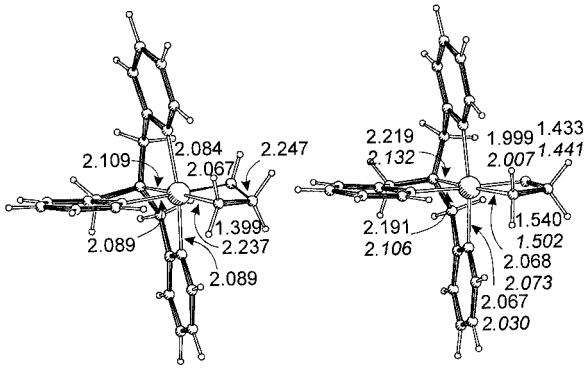

Figure 3. Calculated OH attack transition state and oxetane final product (after deprotonation) for *cis* attack on (tpa)Rh$(C_2H_4)^+$; calculated bond lengths in Å [observed values for (Me-tpa)Rh$(C_2H_4)^+$ [7] in *italics*]

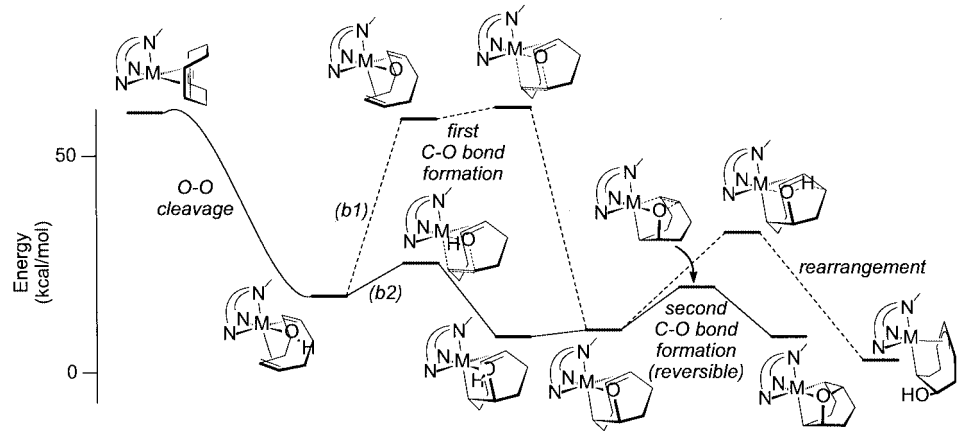

Figure 4. Calculated energy profile [kcal/mol] for *asym* attack at (tpa)Rh(cod)$^+$

and the oxetane final product for the preferred *cis*-to-amine attack on (tpa)Rh$(C_2H_4)^+$.

Figure 4 shows the complete calculated energy profile, including the steps discussed in the following sections, for *asym* (*cis* to the amine group) attack at (tpa)Rh(cod)$^+$.

COD-Derived Oxetanes and Ethers

For COD, the experimentally observed products of the oxidation can be either oxetanes (for M = Ir) or ethers (for M = Rh). We have calculated both types of isomeric products, as well as the transition states for their interconversion, using the *fac*-κ^3-coordinated tpa ligand. We chose this ligand because, depending on the disposition of the nitrogen donor groups around the metal atom, it can displace the remaining C=C bond of the oxetane product, as discussed below.

The results are summarised in Scheme 5. The barriers for ether formation are about 10 kcal/mol for Rh; they represent reactions that would rapidly reach equilibrium at room temperature. The barriers for Ir are slightly larger, as expected. The calculations predict the ether products (***s2***, ***a3***) to be more stable than their oxetane isomers for Rh, whereas for Ir the oxetanes (***s1***, ***a2***) are more stable, in agreement with experiment.

If a tetradentate ligand (tpa) is used in this reaction, it initially has a dangling picolyl group (structures ***s1−2***, ***a1−3***). Depending on the disposition around the metal atom, this can, in some cases, displace the remaining C=C bond of the oxetane product (***s3***, ***a4***). Indeed, for Rh Krom observed displacement in the *sym* isomer but not in the *asym* isomer, whereas for Ir experiment suggests the C=C bond remains coordinated in both isomers.[5] Our calcu-

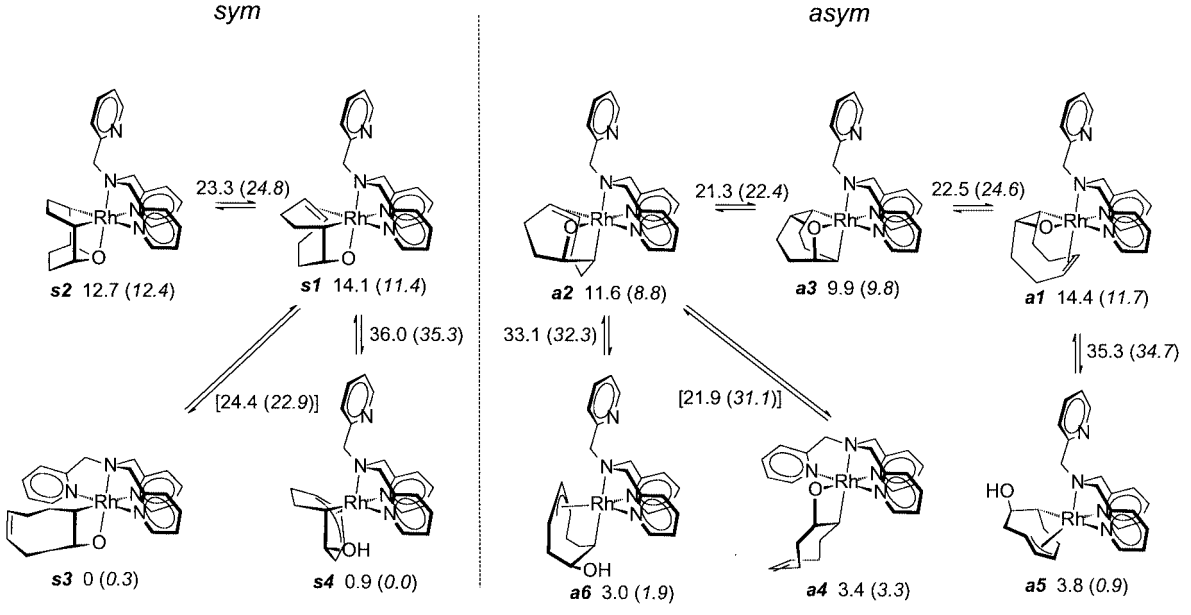

Scheme 5. Calculated relative energies of minima and transition states [kcal/mol] for Rh oxidation products[14] (values for Ir in *italics*)

lations do not agree with this and predict C=C displacement by the dangling Py group to be favourable in all cases. We do not at present have a satisfactory explanation for this discrepancy. It is unlikely to be due to kinetic factors, since even intermediates having both C=C and Py groups detached are predicted to be accessible.[14]

Decomposition of COD-Derived Oxetanes

Experimentally, the oxetane and ether products derived from COD slowly rearrange to hydroxy-enediyl derivatives. This reaction appears to be accelerated by acid, at least for Rh.[3] Here, we have studied the uncatalysed rearrangement, which involves intramolecular transfer of an allylic proton to the oxetane oxygen atom. The calculated barriers (20−25 kcal/mol) are significant but not prohibitive, suggesting that uncatalysed rearrangement would certainly be possible. For Rh in the *asym* series, the path leading to isomer ***a6*** is predicted to be marginally more favourable than that leading to isomer ***a5***; experimentally, isomer ***a5*** is formed exclusively with the dpa ligand. For Ir, the route leading to ***a6*** also has a slightly lower calculated barrier, yet for Me-dpa an isomer of type ***a5*** is still observed experimentally.[4] Obviously, there is no a priori reason why any catalysed rearrangement should have the same selectivity as the uncatalysed reaction.

A Comparison with Ti^{IV}- and Mo^{VI}-Catalysed Epoxidation

It is interesting to contrast the sequence of steps described here to that occurring in olefin epoxidation by H_2O_2 (or ROOH) catalysed by the early transition metals Ti^{IV} [15] and Mo^{VI} (Scheme 6).[16] There, the hydrogen peroxide forms a metal hydroperoxide, from which an oxygen atom is transferred to an olefin without direct metal−olefin coordination. The metal atom activates the OOR group through η^2-coordination, making the OR group a good leaving group,[17] but the metal atom itself is redox-inactive. In the present late-transition-metal case, H_2O_2 oxidizes M^{I} to M^{III}, and this in turn oxidizes the olefin through intramolecular Wacker-type chemistry.[18]

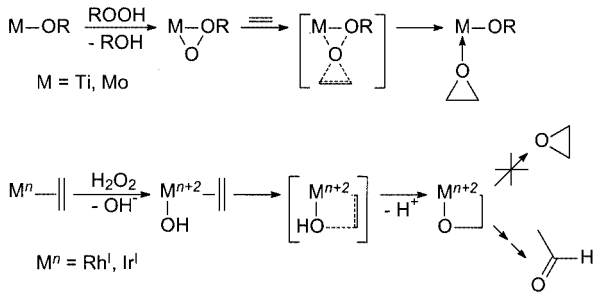

Scheme 6. Comparison of olefin oxidation by peroxides at early and late transition metal atoms

These different mechanisms explain the differences in product types. In Ti^{IV} and Mo^{VI} reactions, the epoxide is the initial product, and unless it is opened in the reaction medium by electrophilic or nucleophilic attack, it will also be the final product. In the type of metal-mediated oxidation chemistry studied here, the initial product is a (protonated) metallaoxetane, from which reductive elimination to the highly strained epoxide would only be expected if the metal atom is in an unusually high oxidation state. That is not the case for Rh^{III} or Ir^{III}, so decomposition to an aldehyde or ketone by β-hydrogen elimination is a more likely outcome.

Conclusions

Calculations have provided a consistent and reasonable picture of the oxidation of $[N_x(olefin)Rh^{I}]^+$ complexes by H_2O_2. The initial step is proposed to be heterolytic O−O cleavage, possibly assisted by hydrogen bonding of, for example, water to the nascent OH^- ion. The next step is probably intramolecular attack of coordinated OH^- on coordinated olefin, followed by loss of a proton. For COD complexes, the oxetanes formed in this way can undergo reversible intramolecular attack of the alkoxide oxygen atom on the remaining C=C bond, leading to ether products. The calculated stabilities and barriers suggest that the products observed experimentally are the thermodynamic ones. For Ir, oxetanes are calculated to be slightly more stable than their ether isomers, but apart from that the differences between Rh and Ir appear to be small.

Table 1. Relative energies [kcal/mol] for oxidation of $(tpa)M(C_2H_4)^+$

	Rh		Ir	
	cis[a]	*trans*[a]	*cis*[a]	*trans*[a]
$(tpa)M(C_2H_4)^+$	66.9		70.2	
H_2O_2 complex	79.6	79.8	82.2	82.3
O−O cleavage TS	93.0	92.8	97.8	95.6
$H_2O_2{\cdot}H_2O$ complex	77.2	80.0	80.6	82.8
O−O cleavage TS	92.1	92.3	96.4	96.6
$(tpa)M(C_2H_4)(OH)^{2+}$[b]	12.9	12.7	7.5	8.4
C_2H_4 insertion TS[b]	17.2	16.7	17.0	16.8
$(tpa)M(CH_2CH_2OH)^{2+}$ [b]	1.9	0.0	1.3	0.0
$(tpa)M(C_2H_4)(O)^+$	55.6	55.3	50.1	52.9
C_2H_4 insertion TS	57.0	55.7	56.7	56.2
$(tpa)M(CH_2CH_2O)^+$	8.3	6.9	8.1	7.3

[a] Position of O attack relative to the amine nitrogen atom. [b] Correction for energies for dicationic species: see Exp. Sect.

Table 2. Relative energies [kcal/mol] for initial step of oxidation of $(dpa)M(cod)^+$ and $(dpa\text{-}Me)M(cod)^+$ by $H_2O_2{\cdot}H_2O$

	Rh		Ir	
	cis[a]	*trans*[a]	*cis*[a]	*trans*[a]
$(dpa)M(cod)^+$	0.0		0.0	
$H_2O_2{\cdot}H_2O$ complex	11.7	10.1	11.1	10.0
O−O cleavage TS	25.6	28.3	25.1	28.5
$(dpa\text{-}Me)M(cod)^+$	0.0		0.0	
$H_2O_2{\cdot}H_2O$ complex	10.9	9.4	11.4	10.3
O−O cleavage TS	24.2	24.8	25.5	25.4

[a] Position of O attack relative to the amine nitrogen atom.

Table 3. Relative energies [kcal/mol] for oxidation of (tpa)M(cod)$^+$

	Rh			Ir		
	cis1[a]	*cis2*[a]	*trans*[a]	*cis1*[a]	*cis2*[a]	*trans*[a]
(κ^3-tpa)M(cod)$^+$		59.6			59.7	
(κ^3-tpa)M(cod)(OH)$^{2+}$[b]	19.0		25.4	11.5		17.5
cod insertion TS[b]	30.7	26.3	31.5	26.8	23.2	27.8
(κ^3-tpa)M(cod-oxetaneH)$^{2+}$ [b]	15.2	10.2	15.5	13.1	6.5	13.1
(κ^3-tpa)M(cod)(O)$^+$	58.0		57.9	49.9		50.6
cod insertion TS	60.7	60.5	58.8	57.2	57.9	56.5
(κ^3-tpa)M(cod-oxetane)$^+$	14.4	11.6	14.4	11.7	8.8	11.4
oxetane-ether TS	22.5	21.3	23.3	24.6	22.4	24.8
(κ^3-tpa)M(cod-ether)$^+$	9.9		12.7	9.8		12.4
H shifts TS	35.3	33.1	36.0	34.7	32.3	35.3
(κ^3-tpa)M(hydroxy-enediyl)$^+$	3.8	3.0	0.9	0.9	1.9	0.0
(κ^3-tpa)M(κ^2-cod-oxetane)$^+$		21.9	24.4		31.1	22.9
(κ^4-tpa)M(κ^2-cod-oxetane)$^+$		3.4	0.0		3.3	0.3

[a] Position of O attack relative to the amine nitrogen atom. *cis1* (*cis2*) has the M−C bond *cis* (*trans*) to the amine nitrogen atom. [b] Correction for energies for dicationic species: see Exp. Sect.

Experimental Section

General Methods: All calculations were carried out with the Turbomole program[19a] coupled to the PQS Baker optimiser.[20] Geometries were fully optimised as minima or transition states at the bp86[21]/RIDFT[22] level using the Turbomole SV(P) basis set[19c][19d] on all atoms (small-core pseudopotential[19c][19e] on Rh and Ir); the nature of each stationary point was then checked by a numerical frequency analysis. Improved energies were obtained from single-point calculations at the b3-lyp level[23] using the TZVP basis[19c][19f] (small-core pseudopotential[19c][19e] on Rh and Ir) and a fine ("m4") integration grid. Solvent corrections were calculated at the b3-lyp/TZVP level using the COSMO solvation model[24] with a dielectric constant of 36.67 (acetonitrile). The final energies cited in the text and figures are free energies obtained by combining these solvation-corrected TZVP results with zero-point energy (ZPE) and thermal corrections (enthalpy and entropy, 273 K, 1 bar) calculated from the bp86/RIDFT frequency analyses. All species were put on common energy scales by adding H_2O_2, H_2O, OH^- etc. where appropriate. Tables 1−3 list the relative free energies for species discussed in the text. Complete listings of total energies are given as Supporting Information (Tables S1−S4).

Relative Energies of Mono- and Dicationic Species: Even with the inclusion of COSMO solvation corrections, the present level of calculation fails to provide realistic *relative* energies for species of different charges, such as occur in our heterolytic cleavage reactions of H_2O_2. This must at least in part be due to the neglect of strong *specific* solute−solvent interactions (e.g., hydrogen bonding) in the solvation model. The error made in the specific case of ionisation of water can be estimated from Equation (1), where $\varepsilon_{H_3O^+}$, ε_{OH^-}, and ε_{H_2O} are calculated at the COSMO/TZVP/b3-lyp level using the dielectric constant of water (80.37).

$$\Delta\varepsilon = \varepsilon_{H_3O^+} + \varepsilon_{OH^-} - 2\varepsilon_{H_2O} - RT\ln K_{H_2O}$$
$$K_{H_2O} = \frac{[H_3O^+][OH^-]}{[H_2O]^2} \approx (18)^2\,10^{-20} \quad (1)$$

As a very rough correction for the charge-separation problem, we subtracted this "fudge factor" from all calculated energies of dicationic species. This probably results in over-stabilisation of the dicationic species, since H_3O^+ is likely to have stronger specific solvent interactions than most other solutes, but at present we do not have a method that is guaranteed to produce more realistic relative energies for charge-separated species.

Acknowledgments

We are grateful to Prof. P. Burger (Hamburg) for providing the coupling module between Turbomole and the PQS optimiser, and to Sabic EPC for financial assistance.

[1] B. de Bruin, M. J. Boerakker, J. J. J. M. Donners, B. E. C. Christiaans, P. P. J. Schlebos, R. de Gelder, J. M. M. Smits, A. L. Spek, A. W. Gal, *Angew. Chem. Int. Ed. Engl.* **1997**, *36*, 2064.
[2] T. C. Flood, M. Iimura, J. M. Perotti, A. L. Rheingold, T. E. Concolino, *Chem. Commun.* **2000**, 1681.
[3] B. de Bruin, J. A. Brands, J. J. J. M. Donners, M. P. J. Donners, R. de Gelder, J. M. M. Smits, A. W. Gal, A. L. Spek, *Chem. Eur. J.* **1999**, *5*, 2921.
[4] R. J. N. A. M. Kicken, PhD Thesis, Nijmegen, **2001**.
[5] M. Krom, PhD Thesis, Nijmegen, **2003**.
[6] B. de Bruin, M. J. Boerakker, R. de Gelder, J. M. M. Smits, A. W. Gal, *Angew. Chem. Int. Ed.* **1999**, *38*, 219.
[7] B. de Bruin, M. J. Boerakker, J. A. W. Verhagen, R. de Gelder, J. M. M. Smits, A. W. Gal, *Chem. Eur. J.* **2000**, *6*, 298.
[8] B. de Bruin, J. A. W. Verhagen, C. H. J. Schouten, A. W. Gal, D. Feichtinger, D. A. Plattner, *Chem. Eur. J.* **2001**, *7*, 416.
[9] V. W. Day, W. G. Klemperer, S. P. Lockledge, D. J. Main, *J. Am. Chem. Soc.* **1990**, *112*, 2033.
[10] (olefin)Rh and -Ir complexes can react with oxygen to form peroxo complexes (see, for example, ref.[2]), which can hydrolyze to hydrogen peroxide. Therefore, many O_2 oxygenations may well involve H_2O_2 as the actual oxidant of the olefin complex (as suggested in ref.[11]).
[11] B. de Bruin, T. P. J. Peters, J. B. M. Wilting, S. Thewissen, J. M. M. Smits, A. W. Gal, *Eur. J. Inorg. Chem.* **2002**, 2671.
[12] We could not always locate transition states for the "sudden-collapse" paths involving only H_2O_2. For the smoother paths using $H_2O_2{\cdot}H_2O$, all relevant transition states were found.
[13] See, for example: T. Cundari, *Chem. Rev.* **2000**, *100*, 807 and references cited therein.
[14] The "transition state energies" given in Scheme 5 for displacement of a COD C=C bond by a picolyl group represent the energies of hypothetical 16e intermediates having *both* the picolyl group and the C=C bond detached from the metal atom.
[15] See, for example: [15a] Y.-D. Wu, D. K. W. Lai, *J. Org. Chem.*

1995, *60*, 673. [15b] Y.-D. Wu, D. K. W. Lai, *J. Am. Chem. Soc.* **1995**, *117*, 11327. [15c] I. V. Yudanov, P. Gisdakis, C. di Valentin, N. Rösch, *Eur. J. Inorg. Chem.* **1999**, 2135.

[16] See, for example: [16a] I. V. Yudanov, C. di Valentin, P. Gisdakis, N. Rösch, *J. Mol. Catal.* **2000**, *A158*, 189. [16b] D. V. Deubel, J. Sundermeyer, G. Frenking, *J. Am. Chem. Soc.* **2000**, *122*, 10101. [16c] D. V. Deubel, J. Sundermeyer, G. Frenking, *Inorg. Chem.* **2000**, *39*, 2314. [16d] D. V. Deubel, J. Sundermeyer, G. Frenking, *Eur. J. Inorg. Chem.* **2001**, 1819.

[17] Assistance by hydrogen-bond formation has also been suggested for Ti^{IV}-catalysed epoxidation: [17a] D. Tantanak, M. A. Vincent, I. H. Hillier, *Chem. Commun.* **1998**, 1031. However, a later solvation study did not show any specific effect of hydrogen bonding on the ease of oxygen transfer: [17b] R. R. Sever, T. W. Root, *J. Phys. Chem.* **2003**, *B107*, 4090.

[18] See also: B. de Bruin, P. H. M. Budzelaar, A. W. Gal, *Angew. Chem.,* accepted.

[19] [19a] R. Ahlrichs, M. Bär, H.-P. Baron, R. Bauernschmitt, S. Böcker, M. Ehrig, K. Eichkorn, S. Elliott, F. Furche, F. Haase, M. Häser, C. Hättig, H. Horn, C. Huber, U. Huniar, M. Kattannek, A. Köhn, C. Kölmel, M. Kollwitz, K. May, C. Ochsenfeld, H. Öhm, A. Schäfer, U. Schneider, O. Treutler, K. Tsereteli, B. Unterreiner, M. von Arnim, F. Weigend, P. Weis, H. Weiss, *Turbomole*, version 5, Theoretical Chemistry Group, University of Karlsruhe, January **2002**. [19b]O. Treutler, R. Ahlrichs, *J. Chem. Phys.* **1995**, *102*, 346. [19c] Turbomole basis set library, *Turbomole*, version 5, see ref.[12a][19d]A. Schäfer, H. Horn, R. Ahlrichs, *J. Chem. Phys.* **1992**, *97*, 2571. [19e] D. Andrae, U. Haeussermann, M. Dolg, H. Stoll, H. Preuss, *Theor. Chim. Acta* **1990**, *77*, 123. [19f] A. Schäfer, C. Huber, R. Ahlrichs, *J. Chem. Phys.* **1994**, *100*, 5829.

[20] [20a] *PQS*, version 2.4, Parallel Quantum Solutions, Fayetteville, Arkansas, USA, **2001** (the Baker optimiser is available separately from PQS upon request). [20b]J. Baker, *J. Comput. Chem.* **1986**, *7*, 385.

[21] [21a] A. D. Becke, *Phys. Rev. A* **1988**, *38*, 3089. [21b] J. P. Perdew, *Phys. Rev. B* **1986**, *33*, 8822.

[22] K. Eichkorn, F. Weigend, O. Treutler, R. Ahlrichs, *Theor. Chem. Acc.* **1997**, *97*, 119.

[23] [23a] C. Lee, W. Yang, R. G. Parr, *Phys. Rev. B* **1988**, *37*, 785. [23b] A. D. Becke, *J. Chem. Phys.* **1993**, *98*, 1372. [23c] A. D. Becke, *J. Chem. Phys.* **1993**, *98*, 5648. [23d] All calculations were performed using the Turbomole functional "b3-lyp", which is not the same as the Gaussian "B3LYP" functional.

[24] A. Klamt, G. Schüürmann, *J. Chem. Soc., Perkin Trans. 2* **1993**, 799.

Received August 7, 2003
Early View Article
Published Online April 7, 2004

